

# Charmonium from Classical Pure SU(3) Yang-Mills Configurations

O. Oliveira\*, R. A. Coimbra†

Centro de Física Computacional, Departamento de Física,  
Universidade de Coimbra, 3004-516 Coimbra, Portugal

July 7, 2018

## Abstract

A generalized Faddeev-Niemi ansatz for the gluon field is discussed. In its simplest parametrization, the ansatz allows a solution of the classical SU(3) Yang-Mills equations. From these solutions a confining potential for heavy quarkonia is defined. The investigation of charmonium spectra proves that the potential is able to reproduce the experimental spectra at the level of 3%. Moreover, charmonium leptonic and strong decays are investigated. The results are in fair agreement with experimental figures and are in line with other quark model calculations.

## 1 Introduction and motivation

Quantum Chromodynamics (QCD) is the theory describing the interaction between quarks and gluons. QCD being a non-abelian gauge theory, besides the quark-gluon interaction includes gluon-gluon interactions. It is expected that these interactions are responsible for the usual baryons and mesons together with exotic states like, for example, glueballs and gluelumps.

In QCD, the basic building blocks are the quark and gluon fields. However, it appears that nature has a preference for baryons and meson states, i.e. colour singlet states, rather than single isolated quarks or exotic states. Quarks seem to be permanently confined within hadrons. The theory provides hints about the quark and gluon confinement mechanism, but a fully explanation is still lacking.

The simplest picture suggesting quark confinement is the singlet potential computed from Wilson loops [1, 2, 3, 4]. This potential can be viewed as the energy between two static colour charges. For large quark separations, the potential grows linearly making it impossible to separate two quarks. In this sense, the singlet potential is a confinement mechanism applicable to heavy

---

\*email: orlando@teor.fis.uc.pt

†email: rita@teor.fis.uc.pt

quarks. For light sector, even the idea of describing the quark-quark interaction via a non-relativistic potential is questionable.

Besides the Wilson singlet potential, two popular confinement mechanisms are the dual Meissner effect [5, 6, 7, 8] and the vortex condensation picture [9, 10, 11, 12, 13]. In both pictures, confinement is explained invoking special types of gluon configurations, namely the condensation of magnetic monopoles in the dual picture and the percolation of colour vortices in the condensation scenario. Although, a considerable amount of work has been done in favour of both mechanisms, their precise confirmation is still missing.

The above described scenarios do not exhaust possible explanations for quark confinement. Many other mechanisms can be found in the literature. Typically, these mechanisms look for certain types of gluon configuration which, in principle, explain why we are not able to detect a free quark. Implicitly, they assume that the origin of confinement is within the pure gauge sector. The success of the quenched approximation in lattice QCD further supports such an idea.

The interaction between heavy quarks, i.e. charm and bottom, can be studied with non-relativistic quark models [14]. Hopefully, the interquark potential [15, 16, 17, 18, 19] should be derived from QCD. In practice, the potentials are either phenomenological or, at best, QCD-motivated. The idea of defining an interquark potential is appealing and, if one could solve the theory, the potential should be related to a given gluon configuration as the Coulomb potential in QED. However, so far, the known solutions of the classical field SU(3) gauge theory, i.e. instantons, do not suggest quark or gluon confinement.

In this paper we construct solutions of the classical field SU(3) Yang-Mills theory, in Minkowsky spacetime, which lead to confining nonrelativistic potentials<sup>1</sup>. The classical solutions are obtained after the introduction of a generalized Cho-Faddeev-Niemi-Shabanov ansatz which, in Landau gauge, allows a parametrization of the gluon field in terms of two vector fields and a scalar field. For such a gluonic field, the classical field equations are essentially a system of coupled QED like equations for the two vector fields and a massless Klein-Gordon equation for the scalar field. The solutions of the coupled equations can be divided into QED like solutions, i.e. plane wave solutions, and exponential growing fields. The later ones will allow to identify a confining potential for heavy quark systems. Although the potential is given by a multipole expansion, in this work only the  $l = 0$  term will be considered. In order to compute its parameters, the potential is compared with the singlet potential computed from the Wilson loop. It comes that, in the range 0.2 - 1 fm, the new potential follows closely the Wilson loop behaviour, with a maximum deviation of about 50 MeV. The differences being both the small ( $\mathcal{O}(1/r)$ ) and large ( $\mathcal{O}(\exp(\Lambda r)/r)$ ) distance behaviours. Moreover, the potential is characterized by a single mass scale  $\Lambda = 228$  MeV, computed together with the other parameters by fitting the singlet potential in the region 0.2 - 1 fm. Being close to the singlet potential, the charmonium is well described by the new potential. Moreover, assuming a pure vector interaction one can define a spin dependent potential which, together

---

<sup>1</sup>See [20, 21] for related work.

with central potential, is able to reproduce experimental spectra with an error of less than 3%. The leptonic and hadronic decays of charmonium are also investigated. The model is in fair agreement with the experimental figures.

The paper is organized as follows, in section 2, for completeness, the generalized Cho-Faddeev-Niemi-Shabanov ansatz proposed previously is discussed, giving particular attention to its simplest parametrization. In section 3, a potential for heavy quarks is motivated and compared with the singlet potential computed from the Wilson loop. The potential parameters are computed fitting the singlet potential in the region 0.2 - 1 fm. In section 4, the charmonium spectra is calculated with the new potential, including the effect of spin-dependent forces. The recently discovered charmonium states and their possible quantum numbers assignment are discussed. Furthermore, discussion of the hadronic decays and leptonic decays of the  $1^{--}$  is performed. Finally, we draw the conclusions and plans for future work in the last section.

## 2 Classical Gluon Fields

For SU(3) the lagrangian density<sup>2</sup> reads

$$\mathcal{L} = -\frac{1}{4} F_{\mu\nu}^a F^{a\mu\nu} \quad (1)$$

where

$$F_{\mu\nu}^a = \partial_\mu A_\nu^a - \partial_\nu A_\mu^a - gf_{abc}A_\mu^b A_\nu^c, \quad (2)$$

and  $A_\mu^a$  are the gluon fields. The classical equations of motion,

$$\partial_\mu F^{\mu\nu} + ig[A_\mu, F^{\mu\nu}] = 0, \quad (3)$$

being a set of non-linear partial differential equations are quite difficult to solve and to compute a solution of (3) it is usual to introduce an ansatz.

Following a procedure suggest in [23], let us consider a real covariant constant field  $n^a$ . From its definition, it follows

$$D_\mu n^a = \partial_\mu n^a + ig(F^c)_{ab} A_\mu^c n^b = 0, \quad (4)$$

where  $F^a$  are the generators of representation to which  $n$  belongs. If one wants to parametrize the gluon field in terms of  $n$ , the scalar field should have, at least, as many color components as  $A_\mu$ . The adjoint representation fullfils such condition and it will be assumed that  $n$  belongs to this representation, then

$$(F^b)_{ac} = -if_{bac}, \quad (5)$$

$$D_\mu n^a = \partial_\mu n^a + gf_{abc} n^b A_\mu^c = 0. \quad (6)$$

Multiplying the last equation by  $n^a$  it follows

$$\partial_\mu (n^a n^a) = 0. \quad (7)$$

---

<sup>2</sup>In this work we use the notation of [22].

From now on it will be assumed that  $n^a n^a = 1$ .

Defining the color projected field

$$C_\mu = n^a A_\mu^a \quad (8)$$

one writes the gluon field as

$$A_\mu^a = n^a C_\mu + X_\mu^a, \quad (9)$$

where  $X$  is orthogonal to  $n$  in the sense

$$n^a X_\mu^a = 0. \quad (10)$$

In order to establish the gauge transformation properties of the various fields, we consider infinitesimal gauge transformations,

$$U(x) = e^{-i\omega(x)} = 1 - i\omega(x) \quad (11)$$

$$\delta A_\mu^a = \frac{1}{g} \partial_\mu \omega^a + f_{abc} \omega^b A_\mu^c \quad (12)$$

$$\delta n^a = f_{abc} \omega^b n^c. \quad (13)$$

For  $C_\mu$ , the transformation rule looks like a ‘‘projected abelian’’ gauge transformation

$$\delta C_\mu = \frac{1}{g} n^a \partial_\mu \omega^a. \quad (14)$$

For  $X_\mu^a$ , the transformation property is non-linear in the field  $n$ . It follows from (9), (12) and (13)

$$\delta X_\mu^a = \frac{1}{g} (\delta^{ab} - n^a n^b) \partial_\mu \omega^b + f_{abc} \omega^b X_\mu^c \quad (15)$$

and

$$\delta (n^a X_\mu^a) = 0. \quad (16)$$

In order to build an usefull ansatz, one can go back to equation (6), replace the gluon field by the decomposition (9), multiply by  $f_{ade} n^e$  and try to solve for the  $X$  field. After some algebra we get

$$f_{abc} n^b \partial_\mu n^c - \frac{2}{3} g X_\mu^a - g (d_{abe} d_{dce} - d_{dbe} d_{ace}) X_\mu^b n^c n^d = 0 \quad (17)$$

after using the SU(3) relation

$$f_{abc} f_{dec} = \frac{2}{3} (\delta_{ad} \delta_{be} - \delta_{ae} \delta_{bd}) + (d_{adc} d_{bec} - d_{bdc} d_{aec}), \quad (18)$$

where

$$d_{abc} = \frac{1}{4} \text{Tr} (\lambda^a \{ \lambda^b, \lambda^c \}) \quad (19)$$

and  $\lambda^a$  are the SU(3) Gell-Mann matrices. Equation (17) allows us to write

$$X_\mu^a = \frac{3}{2g} f_{abc} n^b \partial_\mu n^c + Y_\mu^a \quad (20)$$

and

$$n^a X_\mu^a = n^a Y_\mu^a = 0. \quad (21)$$

The first term of  $X_\mu^a$  is a generalized Faddeev-Niemi ansatz [24]. The simplest non-trivial  $n$  field with norm one can be parametrized as

$$n^a = \delta^{a1} \sin \theta + \delta^{a2} \cos \theta. \quad (22)$$

Then, with the above definitions equation (17) implies the following relations between the  $Y$  fields

$$Y_\mu^2 = Y_\mu^1 \cot \theta, \quad (23)$$

$$Y_\mu^3 = \frac{1}{2g} \partial_\mu \theta, \quad (24)$$

$$Y_\mu^4 = Y_\mu^5 = Y_\mu^6 = Y_\mu^7 = 0, \quad (25)$$

which together with the color space orthogonality condition (21) gives the gluon field

$$A_\mu^a = n^a C_\mu - \frac{\delta^{a3}}{g} \partial_\mu \theta + \delta^{a8} B_\mu; \quad (26)$$

in the last equation we defined  $B_\mu = Y_\mu^8$ . The corresponding gluon field tensor components are

$$F_{\mu\nu}^a = n^a C_{\mu\nu} + \delta^{a8} \mathcal{B}_{\mu\nu}, \quad (27)$$

where

$$C_{\mu\nu} = \partial_\mu C_\nu - \partial_\nu C_\mu, \quad \mathcal{B}_{\mu\nu} = \partial_\mu B_\nu - \partial_\nu B_\mu. \quad (28)$$

For the above gluonic configuration, the classical action is a functional of the vector fields  $C_\mu$  and  $B_\mu$ ,

$$\mathcal{L} = -\frac{1}{4} (\mathcal{C}^2 + \mathcal{B}^2), \quad (29)$$

and the classical equations of motion (3) become QED-like equations

$$\partial^\mu C_{\mu\nu} = 0, \quad \partial^\mu \mathcal{B}_{\mu\nu} = 0. \quad (30)$$

Moreover, the hamiltonian density and the spin tensor are given by the sum of the contributions of two abelian-like theories associated with  $C_\mu$  and  $B_\mu$  fields. Note that the pure gauge theory at the classical level, is independent of  $\theta$ . However, the inclusion of fermions implies a coupling  $\theta$ -fermions. The coupling with  $\theta$  is associated with the first three Gell-Mann matrices and, for configurations with  $C_\mu = B_\mu = 0$  requires only  $\lambda^3$ ; no coupling with the third color component and the coupling to the first two color components have opposite signs.

The computation of classical solutions of the equations for the gluon configuration considered requires gauge fixing. For the Landau gauge<sup>3</sup>, the full set of equations is

$$\partial^\mu C_\mu = 0, \quad \partial^\mu B_\mu = 0, \quad (31)$$

$$\partial^\mu \theta C_\mu = 0, \quad \partial^\mu \partial_\mu \theta = 0. \quad (32)$$

These together with the classical field equations have plane wave solutions characterized by a four momenta  $k$  such that  $k^2 = 0$ , the fields  $C_\mu$  and  $B_\mu$  are polarized perpendicularly to  $k$ ,

$$C_\mu(k, \lambda) = \epsilon_C(k, \lambda) e^{-ikx}, \quad k^\mu \epsilon_C(k, \lambda) = 0, \quad (33)$$

$$B_\mu(k, \lambda) = \epsilon_B(k, \lambda) e^{-ikx}, \quad k^\mu \epsilon_B(k, \lambda) = 0, \quad (34)$$

$$\theta(k) = \theta_0 e^{-ikx}, \quad (35)$$

and the third color component being polarized along  $k$ . Our aim is to identify possible solutions of the classical field equations (31), (32), (30) which can suggest confining solutions. We will not proceed with the discussion of the solutions of the above set of coupled equations but, instead, discuss a particular class of solutions.

For the pure gauge theory, the condition for a finite action/energy solution does not constraint  $\theta$ . Let us consider the simplest non-trivial configuration one could think of, namely  $C_\mu = B_\mu = 0$ . This particular configuration has zero energy and the field equations are reduced to a massless Klein-Gordon equation for  $\theta$  which can be solved by the usual separation of variables. Indeed, writing  $\theta(t, \vec{r}) = T(t)V(\vec{r})$ , it comes

$$\frac{T''(t)}{T(t)} = \frac{\nabla^2 V(\vec{r})}{V(\vec{r})} = \Lambda^2, \quad (36)$$

where  $\Lambda$  is mass scale which is invariant under rescaling of the gluon field. The solutions with  $\Lambda^2 < 0$  are the usual free field solutions. For  $\Lambda = 0$ , the gluon field is linear in time and the spatial part is the usual solution of the Laplace equation. If  $\Lambda^2 > 0$ ,

$$T(t) = A_T e^{\Lambda t} + B_T e^{-\Lambda t} \quad (37)$$

and writing

$$V(\vec{r}) = \sum_{l,m} V_l(r) Y_{lm}(\Omega) \quad (38)$$

where  $Y_{lm}(\Omega)$  are the spherical harmonics, the functions  $V_l(r)$  can be written in terms of the modified spherical Bessel functions of the 1<sup>st</sup>  $I_{l+1/2}(z)$  and 3<sup>rd</sup>  $K_{l+1/2}(z)$  kind, where  $z = \Lambda r$ ,

$$V_l(r) = A_{lm} \frac{I_{l+1/2}(z)}{\sqrt{z}} + B_{lm} \frac{K_{l+1/2}(z)}{\sqrt{z}}. \quad (39)$$

---

<sup>3</sup>For the Coulomb gauge, the first two equations are slightly more complicated but in the third and fourth equation one should replace  $\partial$  by  $\nabla$ , together with other obvious modifications.

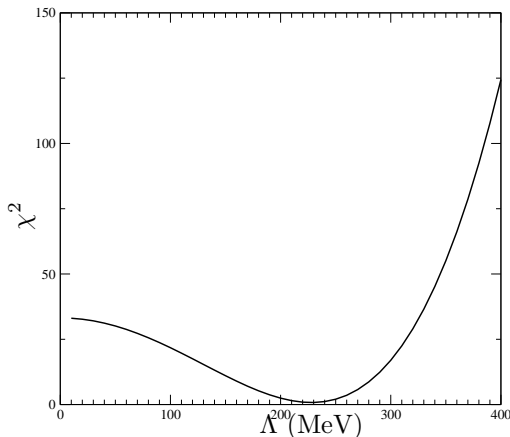


Figure 1: Minima of  $\chi^2$  as function of  $\Lambda$ .

These solutions have the same scale for the temporal and spatial parts and, asymptotically, are real exponential functions. For example, the lowest multipole solution is

$$V_0(r) = A \frac{\sinh(\Lambda r)}{r} + B \frac{e^{-\Lambda r}}{r} \quad (40)$$

and the associated gluon field is

$$A_0^3 = \Lambda (e^{\Lambda t} - b_T e^{-\Lambda t}) V_0(r), \quad (41)$$

$$\vec{A}^3 = -(e^{\Lambda t} + b_T e^{-\Lambda t}) \nabla V_0(r). \quad (42)$$

### 3 A Non-relativistic Potential for Heavy Quarkonium

The coupling of the classical field configuration discussed in the previous section to the fermion fields requires only the  $\lambda^3$  Gell-Mann matrix, i.e.

$$\gamma^\mu \frac{\lambda^3}{2} \partial_\mu \theta \psi; \quad (43)$$

$\psi$  should be understood as a quark Dirac spinor. Assuming that it makes sense to describe the heavy fermion interaction via a potential derived from the above gluon configuration, from the structure of  $\lambda^3$  one naively expects a bound state, let us say the first color component, an unbound state, the second color component and a free particle solution, the third color component. Of course, the usual quark model picture for hadrons is recovered only after gauge transforming all fields.

The classical solution discussed in the last part of the previous section has the same spatial and time scale  $\Lambda = 228 \text{ MeV}$ , i.e. its spatial scale is  $L = 0.865 \text{ fm}$ , while its temporal scale  $T = 2.886 \times 10^{-24} \text{ s}$ .

For charmonium, typical time scales ranges from  $\tau = 1/91 \text{ KeV}^{-1} = 7.2 \times 10^{-21} \text{ s}$  for  $J/\psi(1S)$  up to  $\tau = 8.4 \times 10^{-24} \text{ s}$  for  $\psi(4160)$ .

For bottomonium the time scale ranges from  $\tau = 1.5 \times 10^{-21} \text{ s}$  for  $\Upsilon(1S)$  up to  $\tau = 6.0 \times 10^{-24} \text{ s}$  for  $\Upsilon(10860)$ .

Typical time scales for charmonium and bottomonium are much larger than the time scale of the classical configuration. If quarks propagate in the background of the above classical solution, the effects of propagation should be small, i.e. the quark interactions are almost contact interaction in time. Therefore, in first approximation, the interaction can be parametrized as

$$\delta(t' - t)V(\vec{x}' - \vec{x})\psi(t', \vec{x}')\psi(t, \vec{x}). \quad (44)$$

On the other end, typical wave lengths of charmonium and bottomonium mesons are  $\sim 1/3000 \text{ MeV}^{-1} = 0.07 \text{ fm}$  and  $\sim 1/10000 \text{ MeV}^{-1} = 0.02 \text{ fm}$ , respectively, and they are much smaller than  $L \sim 0.9 \text{ fm}$ . From the point of view of the classical configuration, the mesons are point like structures, i.e. they can be described by a point like wave function  $\phi(\vec{r}, t)$ . Furthermore, if one assumes that charmonium and bottomonium are non-relativistic quark systems, then it seems reasonable to describe the mesons via a gauged Schrödinger equation with a non-relativistic potential given by (38). In first approximation one can forget the contribution from the vector potential of the classical solution.

The non-relativistic potential (38) is not spherical symmetric. However, if only the lowest multipole multipole (40) is considered, one is back to the central potential picture. From now on, we will assume that the confining potential for heavy quarkonium is given by the lowest multipole of the spatial part of  $A_3^0$  and that the Schrödinger equation for heavy mesons is, in first approximation,

$$\left\{ -\frac{\nabla^2}{2m} + V_0(r) \right\} \phi = i\partial_t \phi \quad (45)$$

where  $\phi$  is a heavy meson field and  $m$  the reduced mass of the quarkonium system.

The potential (40) is coulombic for small quark distances

$$V_0(r) = \frac{B}{r}, \quad (46)$$

and confining for large distances

$$V_0(r) = \frac{A}{2r} e^{\Lambda r}; \quad (47)$$

since the potential grows exponentially with distance, it can be viewed as a soft bag model. For large inter-quark distances, the wave function goes to zero as

$$\phi(\vec{r}) \longrightarrow \frac{1}{r} \exp \left\{ -\frac{2}{\Lambda} \sqrt{\frac{mA}{r}} \exp \left[ \frac{\Lambda r}{2} \right] \right\}, \quad \text{for } r \gg 1, \quad (48)$$

with the spatial extension of the quark field becoming smaller for heavier quarks.



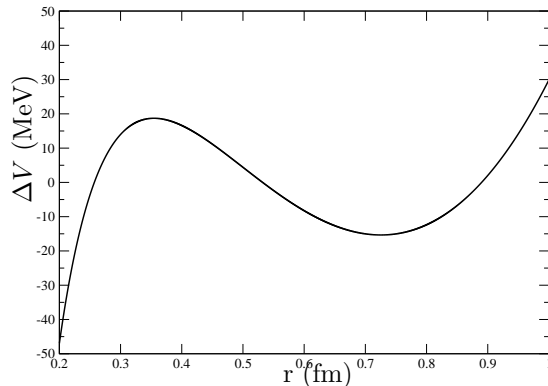


Figure 2:  $\Delta V = V_0(r) - V_{singlet}(r)$ .

The first step towards a proper definition of  $V_0$  as a potential for heavy quark systems is the computation of its various parameters, namely  $A$ ,  $B$  and  $\Lambda$ . This can be done by minimizing the square difference between the new potential and the singlet potential computed from Wilson loops. For the singlet potential we used the results from [3] at  $\beta = 6.4$ . The

$$\chi^2 = \int_{r=0.2fm}^{r=1fm} dr \left[ V_0(r) - V_{singlet}(r) \right]^2 \quad (49)$$

as function of  $\Lambda$  can be seen in figure 1. The curve shows an absolute minimum and we take the potential parameters as their values at this point<sup>4</sup>,

$$A = 11.2542671, \quad B = -0.70113530875, \quad \Lambda = 228.026 \text{ MeV} \quad (50)$$

when  $r$  is measured in  $\text{MeV}^{-1}$ . The difference between  $V_0$  and the lattice potential is reported in figure 2.

It is curious that the value of the only energy scale in the solution is close to standard values for  $\Lambda_{QCD}$ . We have no interpretation for this result. Probably, it is connected to the way the parameters are defined, i.e. to the fit of  $V_0$  to the lattice singlet potential.

## 4 Charmonium - the spectra

The potential  $V_0(r)$  is a first approximation to the full interaction. From the various possible corrections, it will be assumed that the spin-dependent part gives the dominant contribution. Assuming a pure quark-quark vector interaction, the spin potential (see, for example, [55] or [14]) is given by

$$V_{spin} = V_{SO} + V_{ten} + V_{SS}, \quad (51)$$

<sup>4</sup>Assuming that the short distance behaviour of the inter-quark potential is dominated by the one-gluon exchange contribution, then  $B = -4\alpha_s/3$ . The strong coupling constant associated to the fitted value for  $B$  is  $\alpha_s = 0.526$ .

where the spin-orbit  $V_{SO}$ , tensor  $V_{ten}$ , and spin-spin  $V_{SS}$  potentials are

$$V_{SO} = \frac{3}{2m_Q^2} \frac{1}{r} \frac{dV_0}{dr} \vec{L} \cdot \vec{S}, \quad (52)$$

$$V_{ten} = \frac{1}{12m_Q^2} \left( \frac{1}{r} \frac{dV_0}{dr} - \frac{d^2V_0}{dr^2} \right) S_{ten}, \quad (53)$$

$$V_{SS} = \frac{2}{3m_Q^2} \vec{\nabla}^2 V_0 \vec{s}_q \cdot \vec{s}_{\bar{q}}, \quad (54)$$

where  $\vec{L}$  is the orbital angular momentum,  $\vec{s}_Q$  the spin of the heavy quark,  $m_Q$  its mass and

$$S_{ten} = 4 \left[ 3 (\vec{s}_Q \cdot \hat{r}) (\vec{s}_{\bar{Q}} \cdot \hat{r}) - \vec{s}_Q \cdot \vec{s}_{\bar{Q}} \right] \quad (55)$$

is the tensor operator. With the above definitions, the potential verifies the Gromes constraint [25] that arises from the boost invariance of the QCD.

In the following, the mesons states are classified according to the usual spectroscopic notation  $n^{2S+1}L_J$ , where  $S$  is the total spin and  $J$  the total angular momenta. The Schrödinger equation is solved for  $V_0(r)$  with the wave function  $\Psi_{nlm}(\vec{r}) = R_{nl}(r) Y_{lm}(\theta, \phi)$ , where  $n$  is the principal quantum number,  $l$  and  $m$  are the orbital angular momentum and its projection,  $R_{nl}(r)$  is the radial wave function and  $Y_{lm}(\theta, \phi)$  are the spherical harmonic functions. The total wave function is then built by coupling  $\Psi_{nlm}(\vec{r})$  with the spin wave function. The contribution of the spin-dependent potentials will be included perturbatively.

We further define

$$R_{nl}^{(l)}(0) = \frac{d^l R_{nl}(0)}{dr^l}, \quad (56)$$

i.e. the radial wave function and its derivatives at the origin. The various  $R_{nl}^{(l)}(0)$  are required to compute production rates and decays rates.

## 4.1 Quark mass

The charm quark mass,  $m_c$ , was tuned to reproduce the  $\chi_{c2}(1P) - J/\psi(1S)$  mass difference. Using the mesons mass values from the particle data book [26], the mass difference is

$$M(\chi_{c2}(1P)) - M(J/\psi(1S)) = 459.34 \pm 0.11 \text{ MeV} \quad (57)$$

and  $m_c = 1870$  MeV. We have studied other possible definitions for  $m_c$  but although  $m_c$  changes, the meson spectra is essentially the same discussed here.

## 4.2 The spectra

The charmonium radial wave function and its derivatives, for various states, are reported and compared with other quark model calculations in table 1.

For  $S$  wave mesons and for  $V_0$ , the wave function at the origin is essentially constant, except for the state  $1S$ . For the other potentials and for the

	$V_0$	QCD(BT)	Power law	Logarithmic	Cornell
			$ R_{nl}^{(l)}(0) ^2$		
1S	1.739	0.810	0.999	0.815	1.454
2S	1.261	0.529	0.559	0.418	0.927
3S	1.283	0.455	0.410	0.286	0.791
2P	0.248	0.075	0.125	0.078	0.131
3P	0.394	0.102	0.131	0.076	0.186
3D	0.222	0.015	0.026	0.012	0.031

Table 1: Charmonium radial wave function and its derivatives at the origin. All quantities are in  $\text{GeV}^{2l+3}$ . The first column reports the value computed using  $V_0(r)$  and all others are taken from [27]. The references for the various potentials are: QCD(BT) [16], Power law [17], Logarithmic [18], Cornell [19].

states reported in table 1,  $R(0)$  decreases when the principal quantum number increases. This is a major difference between  $V_0$  and the other potentials. For  $V_0$  this means that the decays widths which are sensible to the wave function at the origin, such as the leptonic decays, should scale approximately with the inverse of meson mass squared. For the other potentials this scaling behaviour is not verified. Looking at  $R(0)$ , the potential which is closer to  $V_0$  is the Cornell potential.

For  $P$  mesons, the first derivative of the wave function at the origin increases with the principal quantum number for the QCD inspired potentials  $V_0$ , QCD(BT) and Cornell. The largest increase reported in table 1 happens for  $V_0$ . For the other two potentials,  $|R^{(1)}(0)|^2$  is essentially constant.

For the only  $D$  meson reported in table 1,  $V_0$  shows a second derivative at the origin an order of magnitude larger than all other potentials. Thus,  $V_0$  enhances, for example, the leptonic decay of the  $D$  meson states when compared with all other models.

The full theoretical charmonium spectra is reported in table 2, together with experimental spectra, including the recently discovered charmonium states  $X(3872)$  [28, 29],  $Z(3930)$  ( $\chi_{c2}(2P)$  in the latest version of the Particle Data Book [26]) [30],  $X(3940)$  [31] and  $Y(4260)$  [32]. The experimental values are from the Particle Data Book [26], with the exception of the new states. The meson masses are defined according to

$$M(\text{meson}) = 2m_c + E_{NR} + \Delta_{cc}, \quad (58)$$

where  $E_{NR}$  is the eigenvalue of the Schrödinger equation and  $\Delta_{cc} = -3223$  MeV is a shift introduced to reproduce the  $J/\Psi$  experimental mass value. This mass shift,  $\Delta_{cc}$ , can be viewed as a non-perturbative contribution which is not accessible within the model.

On overall, one can find good agreement between the experimental numbers and the model predictions. The deviations reported in table 2 are below 3 % level.

The quantum numbers of various charmonium states have never been measured experimentally. In the following, we comment on our results and possible quantum number assignments.

#### 4.2.1 $\psi(3836)$

The experimental information on  $\psi(3836)$  is scarce and this state no longer appears in the last particle data book [26]. Only two experiences [34, 35] have seen signs for this meson. The measure of the quantum numbers of  $\psi(3836)$  was discussed in [34]. Based on the comparison with theoretical mass predictions, the authors suggest that it should be a  $^3D_2$  state. Following the same reasoning, from the values of the mesons mass and considering the already excluded quantum numbers, this state can be identified with a  $1^3D_3$ . The mass difference between the prediction and the experimental figures is 5 MeV (0.1%).

#### 4.2.2 $X(3872)$

This particle was discovered by Belle collaboration [36] in the decay  $B^- \rightarrow X(3872)K^-$ , with  $X \rightarrow J/\psi\pi^+\pi^-$ , and confirmed by CDF [37], D0 [38] and BABAR [39] collaborations. Experimentally, only the charge parity  $C = +$  is well established with the data favouring [40, 41, 42] the assignment  $J^{PC} = 1^{++}$ . A  $J^{PC} = 2^{++}$  is not ruled out but seems to be unlikely. In our calculation,  $1^1D_2$ ,  $2^3P_1$ ,  $1^3F_2$  mesons have masses close to the mass of  $X(3872)$  and with  $C = +$ . The assignment with  $2^3P_1$  state shows a deviation from the experimental mass of 67 MeV (1.7%).

#### 4.2.3 The 3940 MeV mass states

Belle collaboration reported on the three possible new states with masses around 3940 MeV:  $X(3940)$  [31],  $Y(3940)$  [43] and  $Z(3930)/\chi_{c2}(2P)$  [30] with measured masses of  $3943 \pm 6 \pm 6$  MeV,  $3940 \pm 11$  MeV and  $3931 \pm 4$  MeV, respectively. The  $X(3940)$  was observed in the process  $e^+e^- \rightarrow J/\psi X$ ,  $Y(3940)$  was seen as a resonance in the decay  $B \rightarrow K\pi\pi J/\psi$  and  $Z(3930)$  was observed in the reaction  $\gamma\gamma \rightarrow D^0\bar{D}^0$ ,  $D^-D^+$ . For the  $Z$  particle, the helicity distribution of the final states particles favors a  $J = 2$  assignment. In the update version of Particle Data Book [26] it appears as a  $\chi_{c2}(2P)$  state with mass value  $3929 \pm 5 \pm 2$ .

Looking at the mass values computed with the model under discussion, the natural candidates are  $2P$  and  $1^3F_2$  levels. For  $Z$ , assuming that it has  $J = 2$  and  $C = +$ , it should be a  $1^3F_2$  charmonium state. The theoretical computed mass shows a deviation from the experimental number of 3 MeV (0.0%).

In what concerns the quantum numbers, for the remaining two states there is no experimental information. Looking at the mass values, the only candidates for  $X(3940)$  and  $Y(3940)$  are  $2^3P_0$  and  $2^1P_1$  states. Since the identification

of  $X$  with a  $\chi_{c1}(2P)$  state has problems [56], one assumes that it is a  $2^1P_1$  state. The theoretical prediction is 111 MeV (deviation of 2.8%) lower than the experimental value. For  $Y(3940)$  the mass suggests a  $\chi_{c0}(2P)$  state. Such state has positive parity state, in agreement with the prediction of [57]. Note that according to these authors,  $X(3940)$  should be one of the following states  $\chi_{c1}(2P)$ ,  $h_c(2P)$  or  $\eta_c(3S)$ . Their analysis favors the  $3^1S_0$  state. For  $Y$  the theoretical prediction is 16 MeV (deviation of 0.4 %) above the value quoted in the particle data book.

#### 4.2.4 $Y(4260)$

This broad resonance was observed in  $e^+e^- \rightarrow \gamma_{ISR}\pi^+\pi^-J/\psi$  with a mass of 4.26 GeV [32], meaning that it has the quantum numbers of the photon  $J^{PC} = 1^{--}$ . From table 2, the closest mass state is the  $3^3S_1$ , which has a mass 96 MeV (deviation of 2.3 %) lower than the measured value.

#### 4.2.5 $\psi(4040)$ , $\psi(4160)$ , $\psi(4415)$

The states  $\psi(4040)$ ,  $\psi(4160)$ ,  $\psi(4415)$  were observed in  $e^+e^- \rightarrow hadrons$  [45]. In what concerns their quantum numbers, there is no experimental information but it is usual to assume that they are vector particles. In what concerns theoretical predictions, there aren't  $1^{--}$  states around the mass value of  $\Psi(4040)$  and  $\Psi(4415)$ . With quantum numbers  $1^{--}$  we can assign the  $\Psi(4160)$  with  $2^3D_1$ .

From table 2 and looking only at the mass values, there a number of states which can be associated with  $\Psi(4040)$  and  $\Psi(4415)$ . For the first state,  $2^3P_2$  and  $1^3F_3$  are good candidates and for  $\Psi(4415)$  the candidates are  $3^3P_1$  and  $3^1P_1$ . Note that, given the difference in mass to the lowest  $1^{--}$  meson, 942 MeV for  $\Psi(4040)$  and 1324 MeV for  $\Psi(4415)$ , a possible interpretation for both states being that they are gluonic excitations rather than quark excitation states. In this sense,  $\Psi(4040)$  should be a bound state of  $J/\Psi$  and the  $J^{PC} = 0^{++}$   $f_0(980)$ , while  $\Psi(4415)$  a bound state of  $J/\Psi$  and the  $J^{PC} = 0^{++}$   $f_0(1324)$ . Given the lack of experimental information, hopefully, only after studying their production and decays will be possible to identify the associated quantum numbers.

### 4.3 Comparison With Other Quark Models and With Lattice QCD

In order to compare our spectra with other charmonium calculations, we reproduce table II from [56] including our figures in table 3 and updating the particle data book figures. In table 3, BGS are the results of a simple non-relativistic quark model [58], GI is an updated version of the ‘‘relativised’’ Godfrey-Isgur model [58], EFG is the relativistic quark model of Ebert, Faustov and Galkin [54], Cornell are the results of the original Cornell model including effects to the coupling to open charm virtual states [19]. CP-PACS [33] and Chen [59] are two lattice calculations in the quenched approximation. For comparison, in the first column we report the Particle Data Book values [26]. Note that in

table, the particle identification assumes the “Standard” notation, i.e.  $3^3S_1$  is identified with  $\Psi(4040)$ ,  $4^3S_1$  with  $\Psi(4415)$  and  $Z(3930)$  with  $\chi_{c2}(2P)$ . From the table it is clear that  $V_0$  as well as the lattice simulations underestimate the hyperfine splittings  $3^3S_1 - 1^3S_0$ . For the lattice this is believed to be due to the quenched approximation - see, for example, [44].

Following [56], in table 4 we report the average model errors using the values reported in table 3. Note that, the particle identification in table 3 does not favor our calculation. Nevertheless, the model predictions are in line with other quark models and provides an overall agreement with the experimental spectra similar to lattice calculations. Of course, an analysis of the meson decays is required to confirm or not the model as a valid model for charmonium.

## 5 Charmonium Decays

In order to further test the heavy quark potential under discussion, we have computed leptonic and hadronic decay widths.

### 5.1 Leptonic Decays

For the leptonic decays we follow the van Royen-Weisskopf [46] approach and assume that QCD corrections can be included perturbatively. Then, the computation of the decay widths requires only the knowledge of the wave function at the origin and its derivatives [47].

For  $n^3S_1$  states, the leptonic width  $\Gamma_{e^+e^-}$  is given by

$$\Gamma_{e^+e^-}^{(0)}(3S_1) = \frac{4e_q^2\alpha^2}{M_{q\bar{q}}^2} |R_{nS}(0)|^2 \quad (59)$$

where  $M_{q\bar{q}}$  is the mass of the  $3^3S_1$  state,  $e_q$  is the electric quark charge (in units of  $|e|$ ),  $\alpha$  the fine structure constant and  $R_{nS}(0)$  the radial wave function of the bound state at the origin.

For  $n^3D_1$  states, the leptonic width is [60, 61]

$$\Gamma_{e^+e^-}^{(0)}(3D_1) = \frac{25e_q^2\alpha^2}{2m_q^4M_{q\bar{q}}^2} |R^{(2)}(0)|^2 \quad (60)$$

where  $R_{3D_1}^{(2)}$  stands for the second derivative of the radial wave function at the origin.

In table 5 we report our predictions for the leptonic widths. In order to avoid the problem of the estimation of QCD corrections, the theoretical widths were computed relative to the  $J/\Psi$  width. The figures reported in table 5 use the particle data book value for

$$\Gamma_{(J/\Psi \rightarrow e^+e^-)} = 5.55 \pm 0.14 \pm 0.02 \text{ keV}. \quad (61)$$

In table 6 our predictions for  $n^3S_1$  widths are compared with other models. All values were computed relatively to the  $J/\Psi$  width and using the experimental value for the meson masses as reported in the Particle Data Book [26]. All models give reasonable estimates for the  $\Psi(2S)$  leptonic width but for the remaining states the leptonic width are clearly overestimated, with  $V_0$  providing always the largest figures. For  $V_0$ ,  $\Psi(4040)$  does not fit into the spectra and therefore the number reported should not compare well with the experimental figure. For  $\Psi(4160)$ , at least in some models, it is expected a large mixing with an S-state which could explain the differences between the theoretical prediction and the experimental measure.

### 5.1.1 Mixing Effects in Charmonium

For  $J^{PC} = 1^{--}$  mesons, the theoretical predictions of the leptonic widths computed using the heavy quark potential  $V_0$  are reported in table 5. For  $\psi(2S)$  the model prediction is larger than the experimental number by a factor of 15%. The model overestimates the widths of  $\psi(3770)$  and  $\psi(4160)$  by a large factor. The deviation can be explained, at least partially, in terms of mixing between states. In the quark model under discussion, the tensor interaction is responsible for the mixing of the S-wave and D-wave central potential states. Indeed,  $\psi(2S)$  a  $2^3S_1$  state,  $\psi(3770)$  a  $1^3D_1$  state and  $Y(4260)$  identified with a  $3^3S_1$  state,  $\Psi(4160)$  identified with a  $2^3D_1$  have the same spin and the same total spin. Moreover, the theoretical mass predictions for such states differ by 29 MeV and 9 MeV, respectively; see table 2.

The perturbative calculation of the mixing induced by the spin-dependent potential improves only very slightly the agreement between theory and experiment. Therefore, the differences are not due to the mixing between the single channel states considered here but mainly to the coupling to open charm channels. In this article we will not perform a coupled channel analysis. Instead, a phenomenological estimate of the mixing for these  $J^{PC} = 1^{--}$  states, parametrizing the mixing via a single parameter [51]

$$|\psi(3770)\rangle = \cos\theta |1^3D_1\rangle + \sin\theta |2^3S_1\rangle, \quad (62)$$

$$|\psi(2S)\rangle = -\sin\theta |1^3D_1\rangle + \cos\theta |2^3S_1\rangle, \quad (63)$$

The leptonic widths are given by [52]

$$\Gamma_{e^+e^-}(\psi(3770)) = \frac{4\alpha^2 e_c^2}{M^2[\psi(3770)]} \left| \sin\theta R_{2S}(0) + \frac{5}{2\sqrt{2}m_c^2} \cos\theta R_{1D}^{(2)}(0) \right|^2 \quad (64)$$

and

$$\Gamma_{e^+e^-}(\psi(2S)) = \frac{4\alpha^2 e_c^2}{M^2[\psi(2S)]} \left| \cos\theta R_{2S}(0) - \frac{5}{2\sqrt{2}m_c^2} \sin\theta R_{1D}^{(2)}(0) \right|^2 \quad (65)$$

where  $\alpha$  is the fine-structure constant and  $e_c$  the charm electric charge. Similar expressions hold for  $Y(4260)$  and  $\Psi(4160)$ . If the QCD corrections are identical

for the two states it comes

$$\frac{M^2[\psi(3770)] \Gamma_{e^+e^-}(\psi(3770))}{M^2[\psi(2S)] \Gamma_{e^+e^-}(\psi(2S))} = \frac{|1.123 \sin \theta + 0.089 \cos \theta|^2}{|1.123 \cos \theta - 0.089 \sin \theta|^2} = 0.092 \pm 0.012 \quad (66)$$

$$(67)$$

Fitting these ratios to the experimental values yields the solutions  $\theta = 12.4^\circ \pm 1.0^\circ$ ,  $-21.4^\circ \pm 1.0^\circ$  and the leptonic decay widths become

	$\Gamma_{e^+e^-}$ no mixing	$\Gamma_{e^+e^-}$ with mixing	$\Gamma_{e^+e^-}$ Exp.
$\psi(2S)$	2.84	2.62	$2.48 \pm 0.06$
$\psi(3770)$	0.02	0.23	$0.219^{+0.028}_{-0.022}$

with all widths in keV. Clearly, the mixing improves the theoretical estimations.

Assuming that  $Y(4260)$  is a  $3^3S_1$  state which mix with  $\Psi(4160)$  a  $2^3D_1$  state, or reversing the assignments, and adjusting the mixing angle to reproduce the experimental width  $\Gamma_{e^+e^-}(\Psi(4160)) = 0.83 \pm 0.07$  keV one obtains  $\Gamma_{e^+e^-}(Y(4260)) = 1.42$  keV in both cases. This calculation is resumed in the following table.

<i>state</i>	<i>assignment</i>	$\Gamma_{e^+e^-}$ no mixing	$\Gamma_{e^+e^-}$ with mixing	$\Gamma_{e^+e^-}$ Exp.
$3^3S_1$	$\Psi(4160)$	2.28	0.83	$0.83 \pm 0.7$
$2^3D_1$	$Y(4260)$	0.04	1.42	
$3^3S_1$	$Y(4260)$	2.16	1.42	
$2^3D_1$	$\Psi(4160)$	0.05	0.83	$0.83 \pm 0.7$

## 5.2 Hadronic widths

In what concern hadronic decays, for  $S$ -wave mesons one can consider the following processes<sup>5</sup>

$$n^1S_0 \rightarrow \gamma\gamma, gg. \quad (68)$$

The theoretical estimates of widths, including QCD corrections, are given by (see, for example [49])

$$\Gamma(^1S_0 \rightarrow \gamma\gamma) = 3e_q^4 \alpha^2 \frac{|R(0)|^2}{m_Q^2} \left(1 - \frac{3.4\alpha_s}{\pi}\right) \quad (69)$$

$$\Gamma(^1S_0 \rightarrow gg) = \frac{2\alpha_s^2}{3} \frac{|R(0)|^2}{m_Q^2} \left(1 + \frac{4.8\alpha_s}{\pi}\right) \quad (70)$$

<sup>5</sup>For  $n^3S_1$  mesons, one can computed theoretical estimates for partial widths for decays into  $\gamma\gamma\gamma$ ,  $ggg$  and  $gg\gamma$ . However, typically,  $^3S_1$  states couple to a large number of hadronic decay channels, which makes the comparison of the theoretical estimates with experimental figures quite difficult. Moreover, the QCD corrections are large and probably the factorisation used in the theoretical calculations does not hold. Indeed, typically, the theoretical figures are quite far away from the experimental values. For these reasons, we do not discuss hadronic widths for  $^3S_1$  mesons.



with the replacement  $m_c = M(\text{meson})/2$ .

For  $n^1S_0$  states, again considering only ratios to the ground state meson, and using the following experimental values for  $\Gamma(\eta_c \rightarrow \gamma\gamma) = 6.7_{-0.8}^{+0.9}$  keV and  $\Gamma(\eta_c \rightarrow gg) = \Gamma_{tot} = 25.5 \pm 3.4$  MeV [26], we obtain the widths reported in table 7. For  $\eta_c(2S)$  the theoretical estimated total width agrees well with the measured value.

For  $P$  wave mesons the decays we consider the following decays

$$\begin{aligned}
n^3P_2 &\longrightarrow \gamma\gamma, gg, \\
n^3P_1 &\longrightarrow q\bar{q}g, \\
n^3P_0 &\longrightarrow \gamma\gamma, gg \\
n^1P_1 &\longrightarrow \gamma\gamma, ggg, gg\gamma.
\end{aligned}
\tag{71}$$

The expressions for the decay widths relevant to  $P$  states, without QCD corrections, are

$$\Gamma(^3P_0 \rightarrow gg) = 6\alpha_s^2 \frac{|R_P^{(1)}(0)|^2}{m_Q^4} \tag{72}$$

$$\Gamma(^3P_0 \rightarrow \gamma\gamma) = 27e_q^4\alpha^2 \frac{|R_P^{(1)}(0)|^2}{m_Q^4} \tag{73}$$

$$\Gamma(^3P_1 \rightarrow q\bar{q}g) = \frac{8n_f\alpha_s^3}{9\pi} \frac{|R_P^{(1)}(0)|^2}{m_Q^4} \ln(m_Q < r >) \tag{74}$$

$$\Gamma(^3P_2 \rightarrow gg) = \frac{8\alpha_s^2}{5} \frac{|R_P^{(1)}(0)|^2}{m_Q^4} \tag{75}$$

$$\Gamma(^3P_2 \rightarrow \gamma\gamma) = \frac{36}{5}e_q^4\alpha^2 \frac{|R_P^{(1)}(0)|^2}{m_Q^4} \tag{76}$$

$$\Gamma(^1P_1 \rightarrow ggg) = \frac{20\alpha_s^3}{9\pi} \frac{|R_P^{(1)}(0)|^2}{m_Q^4} \ln(m_Q < r >) \tag{77}$$

$$\Gamma(^1P_1 \rightarrow gg\gamma) = \frac{36}{5}e_q^2 \frac{\alpha}{\alpha_s} \Gamma(^1P_1 \rightarrow ggg) \tag{78}$$

where  $\langle r \rangle = \int_0^\infty dr r u_{nl}^2(r)$ . The expressions for  $nP$  states are from [49], except (78) which is from [62]. The predicted widths are reported in table 8. In the calculation we have  $\alpha_s = 0.29 \pm 0.03$  (see [53]), neglect QCD corrections and used  $M(\text{state})/2$  rather than  $m_q$  in the formulas, except in the logarithm, where we used  $M(\text{state}) < r >$ . Note that these formulas are rough estimates of the partial widths for the corresponding annihilations processes.

The rates for annihilations of the  $^3D_J$  states into three gluons (via color-singlet operators) are given by [63, 64]

$$\Gamma(^3D_J \rightarrow ggg) = \frac{10\alpha_s^3}{9\pi} C_J \frac{|R_D''(0)|^2}{m_Q^6} \ln(4m_Q < r >) \tag{79}$$

where  $C_J = \frac{76}{9}, 1, 4$ , for  $J = 1, 2, 3$ .

The two-gluon annihilation rate of the  $^1D_2$  state is given by [52]:

$$\Gamma(^1D_2 \rightarrow gg) = \frac{2\alpha_s^2 \alpha_s^3}{3} \frac{|R_D''(0)|^2}{m_Q^6} \quad (80)$$

The values in table 8 are similar to the ones calculated by [62], except for the state  $1^3D_1$  where they used  $M(1^3D_1) = 3872$  MeV, instead of the experimental value.

## 6 Results and Conclusions

In this paper it is proposed a generalized Faddeev-Niemi ansatz for the gluon field - see equations (9), (20) and (21). The ansatz writes the gluon field in terms of two vector fields and a real scalar field in the adjoint representation of SU(3). In its simplest parameterization,  $A_\mu$  is given by (26) and the associated classical equations of motion become abelian-like equations. Moreover, the hamiltonian and spin tensor are the sum of two abelian-like contributions from the two vector fields. In Landau gauge, the solutions of the classical equations of motion can be written as plane waves, with a time-like four momenta, and with the  $A_\mu$  having longitudinal and transverse polarizations. A particular class of solutions with zero classical energy is built. These configurations are asymptotically growing exponential functions in space and in time and are characterized by a unique mass scale. From these solutions, a potential for heavy quark phenomenology is suggested and investigated. In the range of 0.2 - 1 fm, the new potential follows essentially the singlet potential but differ from it for small and large inter-quark separations. The minimization of the square difference between the potentials gives  $\Lambda = 228.0$  MeV.

The potential, including perturbatively the spin dependent contributions, is then used to investigate charmonium. In what concerns the mass spectra, the description is precise up to 3% level. Typically, the difference between the theoretical estimation and measured mass is well below de 100 MeV. However, of the known charmonium states, two mesons do not fit in the model prediction, namely  $\Psi(4040)$  and  $\Psi(4415)$ . Possible interpretations of these particles as charmonium states is suggested but not discussed in detail. A full study of the possibilities raised here for these particles is under way. Despite of the success of the spectra, the hiperfine splitting comes two low in the model. This is seen also in lattice simulations and, in our case, probably comes from fitting the new potential to the lattice single potential. We are currently trying to fit the potential parameters to charmonium spectra. This program is very time consuming but we hope to be able to report the results in a reasonable time scale.

A first study of the mesons decays was performed. In what concerns  $S$ -wave leptonic decays, the new potential describes well the widths of the lower states. For excited states, the identification is not clear and the comparisation with

experimental numbers requires further investigations. The leptonic decays show that, for certain states, mixing is crucial. We have computed perturbatively the mixing induced by the spin-dependent potential. However, the mixing induced by the spin-dependent potential only changes slightly our results. On one hand this shows that our calculation is consistent. On the other hand shows that a coupled channel analysis is required to reproduce the observed behaviour. We are currently starting such a program.

In what concerns the hadronic decays, the model predictions are in reasonable agreement with total widths estimates for  $^1S_0$  and  $P$ -wave mesons.

The results for the charmonium spectrum and decays suggest that the potential and, hopefully, the classical configurations discussed here can teach us something about heavy quarkonium. At least, they seem to provide a starting point for a more elaborated calculation, namely a coupled channel calculation, including possible exotic contributions. We are currently involved in exploring such possibilities and extend the use of the potential to other heavy quarkonium.

## Acknowledgements

R. A. Coimbra acknowledges financial support from Fundação para Ciência e Tecnologia, grant BD/8736/2002.

## References

- [1] K. Wilson, Phys. Rev. **D10** (1974) 2445.
- [2] G. S. Bali, Phys. Rep. **343** (2001) 1 [hep-ph/0001312].
- [3] G. S. Bali, K. Schilling, Phys. Rev. **D47** (1993) 661 [hep-lat/9208028].
- [4] S. Necco, hep-lat/0306005.
- [5] Y. Nambu, Phys. Rev. **D10** (1974) 4662.
- [6] G. 't Hooft, in Proceedings of the EPS International Conference, edited by A. Zichichi, p. 1225 (1976).
- [7] S. Mandelstam, Phys. Rep. **23C** (1976) 245.
- [8] T. Suzuki, K. Ishiguro, Y. Mori, T. Sekido, Phys. Rev. Lett. **94** (2005) 132001 [hep-lat/0410001].
- [9] G. 't Hooft, Nucl. Phys. **B138** (1978) 1.
- [10] J. M. Cornwall Nucl. Phys. **B157** (1979) 392.
- [11] H. B. Nielsen, P. Olesen, Nucl. Phys. **B160** (1979) 380.
- [12] L. Del Debbio, M. Faber, J. Greensite, Š. Olejnik, Phys. Rev. **D55** (1997) 2298.

- [13] M. Quandt, H. Reinhardt, M. Engelhardt, PoS(LAT2005)320 [hep-lat/0509114].
- [14] See, for example, J. F. Donoghue, E. Golowich, B. R. Holstein, T. Ericson, *Dynamics of the Standard Model*, CUP 1994, and references therein.
- [15] J. Richardson, Phys. Lett. **B82** (1979) 272.
- [16] W. Buchmüller, S.-H. H. Tye, Phys. Rev. **D24** (1981) 132.
- [17] A. Martin Phys. Lett. **B93** (1980) 338.
- [18] C. Quigg, J. L. Rosner, Phys. Lett. **B71** (1977) 153.
- [19] E. Eichten, K. Gottfried, T. Kinoshita, K. D. Lane, T.-M. Yan, Phys. Rev. **D17** (1978) 3090; **D21** (1978) 313(E); **D21** (1980) 203.
- [20] O. Oliveira, R. A. Coimbra, hep-ph/0305305.
- [21] O. Oliveira, Aip Conf. Proc, **756** (2005) 375.
- [22] K. Huang, *Quarks, Leptons & Gauge Fields*, World Scientific, 1992.
- [23] Y. M. Cho, Phys. Rev. **D62** (2000) 074009.
- [24] L. Faddeev, A. J. Niemi, Phys. Lett. **B464** (1999) 90.
- [25] D. Gromes, *Z. Phys.* **C26** (1984) 401.
- [26] W.-M. Yao *et al.*, Journal of Physics **G33** (2006) 1
- [27] E. J. Eichten, C. Quigg, Phys. Rev. **D52** (1995) 1726.
- [28] K. Abe *et al.* (Belle Collaboration), hep-ex/0505037.
- [29] K. Abe *et al.* (Belle Collaboration), hep-ex/0505038.
- [30] K. Abe *et al.* (Belle Collaboration), hep-ex/0507033.
- [31] K. Abe *et al.* (Belle Collaboration), hep-ex/0507019.
- [32] B. Aubert *et al.* (Babar Collaboration), Phys. Rev. Lett. **95** (2005) 142001 [hep-ex/0506081].
- [33] M. Okamoto *et al.* (CP-PACS Collaboration), Phys. Rev. **D65** (2002) 094508.
- [34] L. Antoniazzi *et al.* (E705 Collaboration), Phys. Rev. **D50** (1994) 4258.
- [35] J. Z. Bai *et al.* (BES Collaboration), Phys. Rev. **D57** (1998) 3854.
- [36] S. -K. Choi *et al.* (Belle Collaboration), Phys. Rev. Lett. **91** (2003) 262001.
- [37] D. Acosta *et al.* (CDF Collaboration), Phys. Rev. Lett. **93** (2004) 072001.

- [38] V. M. Abazov *et al.* (D0 Collaboration), *Phys. Rev. Lett.* **93** (2004) 162002.
- [39] B. Aubert *et al.* (BABAR Collaboration), *Phys. Rev.* **D71** (2005) 071103.
- [40] See E. Swanson, hep-ph/0509237 and references therein.
- [41] See C. Quigg *PoS (HEP2005)* 400 [hep-ph/0509332] and references therein.
- [42] See T. Lesiak hep-ex/0511003 and references therein.
- [43] S. -K. Choi *et al.* (Belle Collaboration), *Phys. Rev. Lett.* **94** (2005) 182002.
- [44] K. J. Juge, A. Cais, M. B. Oktay, M. J. Peardon, S. M. Ryan, *PoS (LAT2005)* 029.
- [45] See [26] and references therein.
- [46] R. van Royen, V. F. Weisskopf, *Nuovo Cimento* **50** (1967) 617; **51** (1967) 583.
- [47] See [48], [49] and [50] for the expressions for the various decay widths, including QCD corrections.
- [48] W. Kwong, J. L. Rosner, *Ann. Rev. Nucl. Part. Sci.* **37** (1987) 325.
- [49] W. Kwong, P. B. Mackenzie, R. Rosenfeld, J. L. Rosner, *Phys. Rev.* **D37** (1988) 3210.
- [50] L. Köpke, N. Wermes, *Phys. Rep.* **174** (1989) 67.
- [51] J. L. Rosner, *Phys. Rev.* **D64** (2001) 094002.
- [52] V. A. Novikov *et al.*, *Phys. Rep.* **41C** (1978) 1.
- [53] K. K. Seth (CLEO Collaboration), hep-ex/0512039.
- [54] D. Ebert, R. N. Faustov, V. O. Galkin, *Phys. Rev.* **D67** (2003) 014027 (2003) [arXiv:hep-ph/0210381].
- [55] W. Lucha, F. F. Schoberl, D. Gromes, *Phys. Rep.* **200** (1991) 127
- [56] E. S. Swanson, *Phys.Rept.* **429** (2006) 243, hep-ph/0601110.
- [57] S. S. Gershtein, A. K. Likhoded, A. V. Luchinsky, *Phys. Rev.* **D74** (2006) 016002
- [58] T. Barnes, S. Godfrey and E. S. Swanson, *Phys. Rev.* **D72** (2005) 054026
- [59] P. Chen, *Phys. Rev.* **D64** (2001) 034509.
- [60] T. Barnes, *Charmonium at BES and CLEO-c*, Expanded version of an invited presentation to the CLEO-c and BESIII Joint Workshop on Charm, QCD and Tau Physics (Beijing, 13-15 Jan 2004), arXiv:hep-ph/0406327

- [61] P. Gonzalez *et al.*, Phys. Rev. D **68**, 034007 (2003)
- [62] T. Barnes and S. Godfrey, Phys. Rev. D **69** (2004) 054008
- [63] G. Bélanger and P. Moxhay, Phys. Lett.B **199** (1987) 575
- [64] W. Kwong, J. L. Rosner, Phys. Rev. D **38** (1988) 279.

state	Theory	Particle	Experimental	deviation (MeV)
$1^3S_1$	3097*	$J/\Psi(1S)$	$3096.916 \pm 0.011$	
$1^1S_0$	3075	$\eta_c(1S)$	$2980.4 \pm 1.2$	95
$1^3P_2$	3556*	$\chi_{c2}(1P)$	$3556.26 \pm 0.11$	
$1^3P_1$	3462	$\chi_{c1}(1P)$	$3510.59 \pm 0.10$	-49
$1^3P_0$	3372	$\chi_{c0}(1P)$	$3415.16 \pm 0.35$	-43
$1^1P_1$	3478	$h_c(1P)$	$3525.93 \pm 0.27$	-48
$2^3S_1$	3659	$\Psi(2S)$	$3686.093 \pm 0.034$	-27
$2^1S_0$	3633	$\eta'_c(2S)$	$3638 \pm 4$	-5
$1^3D_3$	3841	$\Psi(3836)$	$3836 \pm 13$	5
$1^3D_2$	3755			
$1^3D_1$	3688	$\Psi(3770)$	$3771.1 \pm 2.4$	83
$1^1D_2$	3754			
$2^3P_2$	4048			
$2^3P_1$	3938	$X(3872)$	$3871.2 \pm 0.6$	67
$2^3P_0$	3832	$Y(3940)$	$3943 \pm 17$	-111
$2^1P_1$	3959	$X(3940)$	$3943 \pm 8$	16
$1^3F_4$	4114			
$1^3F_3$	4012			
$1^3F_2$	3932	$\chi_{c2}(2P)$	$3929 \pm 5 \pm 2$	3
$1^1F_3$	4007			
$3^3S_1$	4164	$Y(4260)$	$4260 \pm 10$	-96
$3^1S_0$	4135			
$2^3D_3$	4327			
$2^3D_2$	4230			
$2^3D_1$	4155	$\Psi(4160)$	$4153 \pm 3$	2
$2^1D_2$	4230			
$1^3G_5$	4382			
$1^3G_4$	4260			
$1^3G_3$	4161			
$1^1G_4$	4253			
$3^3P_2$	4546			
$3^3P_1$	4422			
$3^3P_0$	4300			
$3^1P_1$	4446			
$2^3F_4$	4603			
$2^3F_3$	4492			
$2^3F_2$	4406			
$2^1F_3$	4487			
$4^3S_1$	4669			
$4^1S_0$	4638			
$3^3D_3$	4825			
$3^3D_2$	4719			
$3^3D_1$	4636			
$3^1D_2$	4720			
$2^3G_5$	4877			
$2^3G_4$	4747			
$2^3G_3$	4641			
$2^1G_4$	4740			

Table 2: Charmonium spectrum up to 5000 MeV. The table includes only  $L \leq 4$  states. The quantum states with \* where used to set the model parameters ( $m_c$ ,  $\Delta_{cc}$ ).

State	PDG	$V_0$	BGS	GI	EFG	Cornell	CP-PACS	Chen
$J/\Psi(1^3S_1)$	$3096.916 \pm 0.011$	3097	3090	3098	3096	3095	$3085 \pm 1$	$3084 \pm 4$
$\eta_c(1^1S_0)$	$2980.4 \pm 1.2$	3075	2982	2975	2979	3095	$3013 \pm 1$	$3014 \pm 4$
$\Psi'(2^3S_1)$	$3686.093 \pm 0.034$	3659	3672	3676	3686	3684	$3777 \pm 40$	$3780 \pm 43$
$\eta_c(2^1S_0)$	$3638 \pm 4$	3633	3630	3623	3588	3684	$3739 \pm 46$	$3707 \pm 20$
$\Psi(3^3S_1)$	$4039 \pm 1$	4164	4072	4100	4088	4225	-	-
$\eta_c(3^1S_0)$		4135	4043	4064	3991	4110	-	-
$\Psi(4^3S_1)$	$4421 \pm 4$	4669	4406	4450	-	4625	-	-
$\eta_c(4^1S_0)$		4638	4384	4425	-	4460	-	-
$\chi_2(1^3P_2)$	$3556.20 \pm 0.09$	3556	3556	3550	3556	3523	$3503 \pm 24$	$3488 \pm 11$
$\chi_1(1^3P_1)$	$3510.66 \pm 0.07$	3462	3505	3510	3510	3517	$3472 \pm 9$	$3462 \pm 15$
$\chi_0(1^3P_0)$	$3414.76 \pm 0.35$	3372	3424	3445	3424	3522	3408	$3413 \pm 10$
$h_c(1^1P_1)$	$3525.93 \pm 0.27$	3478	3516	3517	3526	3519	$3474 \pm 40$	$3474 \pm 20$
$\chi_2(2^3P_2)$	$3929 \pm 5 \pm 2$	4048	3972	3979	3972	-	$4030 \pm 180$	-
$\chi_1(2^3P_1)$		3938	3925	3953	3929	-	$4067 \pm 105$	$4010 \pm 70$
$\chi_0(2^3P_0)$		3832	3852	3916	3854	-	$4008 \pm 122$	$4080 \pm 75$
$h_c(2^1P_1)$		3959	3934	3956	3945	-	$4053 \pm 95$	$3886 \pm 92$
$\chi_2(3^3P_2)$		4546	4317	4337	-	-	-	-
$\chi_1(3^3P_1)$		4422	4271	4317	-	-	-	-
$\chi_0(3^3P_0)$		4300	4202	4292	-	-	-	-
$h_c(3^1P_1)$		4446	4279	4318	-	-	-	-
$\Psi_3(1^3D_3)$		3841	3806	3849	3815	3810	-	$3822 \pm 25$
$\Psi_2(1^3D_2)$		3755	3800	3838	3811	3810	-	$3704 \pm 33$
$\Psi_1(1^3D_1)$	$3771.1 \pm 2.4$	3688	3785	3819	3798	3755	-	-
$\eta_{c2}(1^1D_2)$		3754	3799	3837	3811	3810	-	$3763 \pm 22$
$\Psi_3(2^3D_3)$		4327	4167	4217	-	4190	-	-
$\Psi_2(2^3D_2)$		4230	4158	4208	-	4190	-	-
$\Psi_1(2^3D_1)$	$4153 \pm 3$	4155	4142	4194	-	4230	-	-
$\eta_{c2}(2^1D_2)$		4230	4158	4208	-	4190	-	-
$\chi_4(1^3F_4)$		4114	4021	4095	-	-	-	-
$\chi_3(1^3F_3)$		4012	4029	4097	-	-	-	$4222 \pm 140$
$\chi_2(1^3F_2)$		3932	4029	4092	-	-	-	-
$h_{c3}(1^1F_3)$		4007	4026	4094	-	-	-	$4224 \pm 74$
$\chi_4(2^3F_4)$		4603	4348	4425	-	-	-	-
$\chi_3(2^3F_3)$		4492	4352	4426	-	-	-	-
$\chi_2(2^3F_2)$		4406	4351	4422	-	-	-	-
$h_{c3}(2^1F_3)$		4487	4350	4424	-	-	-	-
$\Psi_5(1^3G_5)$		4382	4214	4312	-	-	-	-
$\Psi_4(1^3G_4)$		4260	4228	4320	-	-	-	-
$\Psi_3(1^3G_3)$		4161	4237	4323	-	-	-	-
$\eta_{c4}(1^1G_4)$		4253	4225	4317	-	-	-	-

Table 3: Quark models and lattice charmonium spectra.



$V_0$	BGS	GI	EFG	Cornell	CP-PACS	Chen
1.7%	0.3%	0.6%	0.4%	1.8%	1.5%	1.4%
0.6%	0.1%	0.2%	0.2%	0.7%	0.6%	0.5%

Table 4: Average Model Errors. The first line is the average error. The second line is the square root of the sum of the relative deviations squared, divided by the number of states.

	$ R_{nl}^{(l)}(0) ^2$	$\Gamma_{theo}$	assign.	$\Gamma_{exp}$
$2^3S_1$	1.261	2.84	$\Psi(2S)$	$2.48 \pm 0.06$
$3^3S_1$	1.283	2.26		
		2.28	$\Psi(4160)$	$0.83 \pm 0.07$
		2.16	$\Psi(4260)$	—
$4^3S_1$	1.350	1.90		
$1^3D_1$	0.031	0.02	$\Psi(3770)$	$0.219^{+0.028}_{-0.022}$
$2^3D_1$	0.101	0.05	$\Psi(4160)$	$0.83 \pm 0.07$
$3^3D_1$	0.222	0.08		

Table 5: Theoretical leptonic widths relatively to the experimental value  $\Gamma_{e^+e^-}(J/\Psi)$  in keV. The experimental numbers are from Particle Data Book. The second column reports the charmonium squared radial wave function and its derivatives at the origin in  $\text{GeV}^{3+l}$ . In the widths assign to a given known particle, in the computation of the width it was used the experimental meson mass rather than the theoretical prediction.

	$V_0$	QCD (BT)	Power Law	Log	Cornell	Exp.
$J/\psi(1S)$						
$\rightarrow l^+l^-$ (keV)	—	—	—	—	—	$5.55 \pm 0.14 \pm 0.02$
$\psi(2S)$						
$\rightarrow l^+l^-$ (keV)	2.84	2.55	2.19	2.00	2.50	$2.48 \pm 0.06$
$\psi(4040) [3^3S_1]$						
$\rightarrow l^+l^-$ (keV)	2.41	1.84	1.34	1.15	1.77	$0.86 \pm 0.07$
$\psi(4160) [3^3D_1]$						
$\rightarrow l^+l^-$ (keV)	2.28	1.73	1.27	1.08	1.68	$0.83 \pm 0.07$

Table 6: Charmonium leptonic decay widths in keV.

Level	Final state	Predicted width	Measured width
$2^1S_0$	gg	12.4 (MeV)	$14 \pm 7$ (MeV)
	$\gamma\gamma$	3.26 (keV)	
$3^1S_0$	gg	9.77 (MeV)	
	$\gamma\gamma$	2.57 (keV)	

Table 7:  $n^1S_0$  widths. In the calculation, for  $2^1S_0$  we have used the experimental mass, while for the  $3^1S_0$  we used the predicted mass value. The measured width reported is the total particle width.

Level	assign.	Final state	Predicted width	Measured width
$1^3P_0$	$\chi_{c0}(1P)$	gg	7.22 (MeV)	$10.4 \pm 0.7$ (MeV) (a)
		$\gamma\gamma$	4.06 (keV)	
$1^3P_1$	$\chi_{c1}(1P)$	$q\bar{q}g$	86.2 (keV)	$0.89 \pm 0.05$ (MeV) (a)
$1^3P_2$	$\chi_{c2}(1P)$	gg	1.63 (MeV)	$1.55 \pm 0.11$ (MeV) (b)
		$\gamma\gamma$	921 (eV)	
$1^1P_1$	$h_c(1P)$	ggg	71.5 (keV)	< 1 (MeV) (a)
		gg $\gamma$	5.76 (keV)	
$2^3P_0$	$Y(3940)$	gg	8.27 (MeV)	$87 \pm 22 \pm 26$ (eV) (a)
		$\gamma\gamma$	4.66 (keV)	
$2^3P_1$	$X(3872)$	$q\bar{q}g$	0.103 (MeV)	< 2.3 (MeV) (a)
$2^3P_2$		gg	1.99 (MeV)	
		$\gamma\gamma$	1.12 (keV)	
$2^1P_1$	$X(3940)$	ggg	84.7 (keV)	
		gg $\gamma$	6.82 (keV)	
$1^3D_1$	$\Psi(3770)$	ggg	0.63 (keV)	$23.0 \pm 2.7$ (MeV) (a)
$1^3D_2$		ggg	0.08 (keV)	
$1^3D_3$		ggg	0.27 (keV)	
$1^1D_2$		gg	0.62 (keV)	

Table 8:  $P$ -wave and  $D$ -wave widths. In the calculation for the meson mass we used the experimental values of the particle assigned. When no assignment is given, for the meson mass we use the theoretical prediction. (a) a total width; (b) see [53] - the value decreases if one includes radiative corrections.